THREE-DIMENSIONAL CHARACTERISTICS OF THE COHERENT FINE SCALE EDDY IN TURBULENCE

M. Ashraf Uddin[1], Mamoru Tanahashi[2] and Toshio Miyauchi[2]
[1]Department of Mathematics, Shahjalal University of Science & Technology
Sylhet-3114, Bangladesh.
[2]Department of Mechanical and Aerospace Engineering, Tokyo Institute of Technology,
2-12-1 O-okayama, Meguro-ku, Tokyo 152-8552, Japan
E-mail: auddin-mat@sust.edu

Abstract: *This paper presents the three-dimensional characteristics of coherent fine scale eddies related to their axis in homogeneous isotropic turbulence in order to understand the detailed features of the fine scale eddy in turbulence. The coherent fine scale eddy and their axis are identified by an auto tracking algorithm from the Direct Numerical Simulation (DNS) database, where DNS is performed based on a spectral method. It is shown that the axis of each fine scale eddy contains several nodes, in which these nodes are identified by the minima of second invariant (Q) of the velocity gradient tensor on the axis. It is also shown that the number of nodes increases for strong and relatively long eddy but it decreases for weak and short eddy. At each node the axis bends with a large angle. The maximum azimuthal velocity and axial velocity of coherent fine scale eddy show relatively large fluctuations along their axis, while the diameter is nearly constant along the entire axis of the fine scale eddy. The coherent fine scale eddies have large advection velocity but the dissipation rate along the axis of the eddy is not so large.*

Keywords: *Homogeneous Isotropic Turbulence, Direct Numerical Simulation, Local Flow Pattern, Velocity Gradient Tensor, Second Invariant, Tube-Like Vortical Structure.*

1. Introduction

Active researchers are making their efforts to construct a comprehensive theory for understanding the physical characteristics of tur b u l e n c e for many decades. Especially the studies on fine scale structure in turbulent flows have been the subjects of considerable interest among turbulence researchers. In the theoretical study, it is believed that tube-like structure is a type of eddy or vortex, which is the candidate of fine scale structure, particularly, in the small-scale motions in turbulence[(1)-(4)] Nowadays, from direct numerical simulation of turbulence[(5)-(14)], fine scale tube-like eddy in homogeneous turbulence can be observed, and the visualization of this small-scale structure in the turbulent flow in principle becomes easier. Since direct numerical simulations (DNS) provide vast amount of information, an efficient method is needed to identify the fine scale structure in small scales of turbulence from the DNS database. In recent studies, by direct use of 'local flow pattern' in turbulence[(10)-(12)], the cross-sections of tube-like coherent fine scale eddies are investigated from DNS database of homogeneous isotropic turbulence in which the cross-sections are selected to include the local maximum of second invariant of the velocity gradient tensor on the axis of the fine scale tube-like eddies. In these studies, they have shown that the mean diameter of the coherent fine scale eddies is about 10 times of Kolmogorov microscale (η) and the maximum of mean azimuthal velocity is about a half of *root man square* of velocity fluctuations (u_{rms}) and that the Reynolds numbers dependence of these characters is very weak. The same analyses have been applied to turbulent mixing layer[(15)] and showed that the characteristics of tube-like eddies in homogeneous isotropic turbulence and fully-developed turbulent mixing layer obey the same scaling law. Since the educed fine scale eddies in their study have similar mean azimuthal velocity profiles and distinct axes, they described these eddies as 'coherent fine scale structures' in turbulence. The characteristics of vortical structures in turbulent channel flows[(16)] and MHD turbulence[(17)] also show the similar behavior of tube-like eddies in homogeneous isotropic turbulence. These results suggest that the existence of 'coherent fine scale eddy' in turbulence is universal.

As we discussed above 'coherent fine scale eddies' are the universal structures in turbulence, whereas these structures show strong three-dimensionality in the flow fields. However, three-dimensional characters of these tube-like eddies are hardly discussed in the previous researches. But the lack of the proper

knowledge about this fine scale motions prevents the development of turbulence theory and turbulent models. To understand the detail of fine scale motions of turbulence, investigation of three-dimensional features of coherent fine scale eddies is required. In our previous studies[11],[12], by tracing the axis of the coherent fine scale eddy, we have investigated the three-dimensional features of the fine scale eddy with its' scaling in homogeneous isotropic turbulence. However, it is necessary to clarify the characteristics of each tube-like eddy individually to understand the significant structures and self-stretching behaviors of the fine scale tube-like eddy, and that is the considerable interest of the present study.

Therefore, in this study, we present the individual characteristics of several typical coherent fine scale eddies related to its' axis in homogeneous isotropic turbulence. The objective is to clarify the three-dimensional characteristics of coherent fine scale eddy clearly and quantitatively.

2. Nomenclature

A_{ij} : velocity gradient tensor
l : Integral length scale
s : coordinates along the axis
s_l : coordinates along the axis normalized by l
s_λ : coordinates along the axis normalized by λ
Q : second invariant of velocity gradient tensor
R : third invariant of the velocity gradient tensor
Re_l : Integral length scale Reynolds number
Re_λ : Taylor microscale Reynolds number
r : radius of the fine scale eddy
S_{ij} : symmetric part of the velocity gradient tensor
u_{rms} : root mean square of velocity fluctuations
u_θ : azimuthal velocity
W_{ij} : asymmetric part of the velocity gradient tensor
ε :dissipation rate
ϕ : inclination angle
λ : Taylor microscale
η : Kolmogorov microscale
ν : kinematic viscosity
π : periodic length

3. Identification of the Axis of Coherent Fine Scale Eddy

3.1 DNS database

In this study, DNS data of decaying homogeneous isotropic turbulence has been used, which is calculated by using 256^3 grid points. Reynolds numbers based on u_{rms} and Taylor microscale, λ, of the DNS data is Re_λ=37.1, while Reynolds number based on u_{rms} and Integral length scale, l, of the DNS data is Re_l =190. A spectral method is used for conducting the direct numerical simulations. The aliasing errors due to nonlinear interactions are fully removed by a 3/2-rule. Details of the numerical procedure and conditions of this simulation are given in the recent papers by Tanahashi et al.[11],[12] and Uddin et al.[13],[14].

3.2. Invariants of velocity gradient tensor and coherent fine scale eddy

The concept usually associated with an eddy is that of a region in the flow where the fluid elements are rotating around a 'set of points'. Identification of the eddy or vortex from DNS database is a very difficult and complex task, requiring considerable computational efforts with a proper identification method. There are several methods for identification of the vortical structures in turbulence with significant differences[18] and most of them show *threshold* dependence. We discussed in the introduction that direct 'local flow pattern'[19] can educe coherent structures in several flow fields[10]-[17], which shows universal characteristics in turbulence. This 'local flow pattern' method is completely independent from any *thresholds* of variables. In our previous studies[13],[20], using this method we also have identified the coherent fine scale eddies and its' axes without using any *thresholds* and then discussed the spatial distribution of coherent fine scale eddies by visualization of axes in homogeneous isotropic turbulence. From the distributions of second and third invariants of the velocity gradient tensor one can easily define the 'local flow pattern' in turbulence.

The second and third invariants of the velocity gradient tensor are defined as:

$$Q = -\frac{1}{2}\left(S_{ij}S_{ij} - W_{ij}W_{ij}\right) \tag{1}$$

$$R = -\frac{1}{3}\left(S_{ij}S_{jk}S_{ki} + 3W_{ij}W_{jk}S_{ki}\right) \tag{2}$$

where,

$$S_{ij} = \frac{1}{2}\left(\frac{\partial u_i}{\partial x_j} + \frac{\partial u_j}{\partial x_i}\right) \tag{3}$$

$$W_{ij} = \frac{1}{2}\left(\frac{\partial u_i}{\partial x_j} - \frac{\partial u_j}{\partial x_i} \right) \quad (4)$$

are the symmetric and asymmetric part of the velocity gradient tensor:

$$A_{ij} = \frac{\partial u_i}{\partial x_j} = S_{ij} + W_{ij} \quad (5)$$

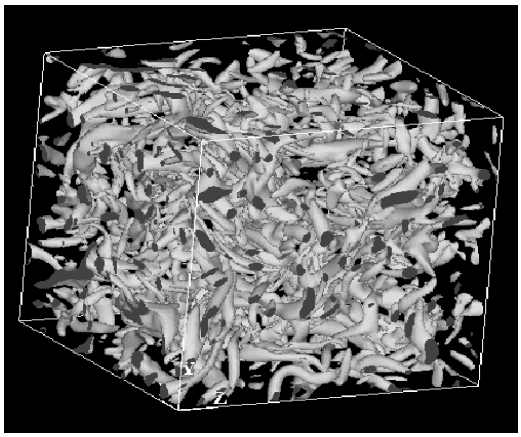

Fig. 1: Contour surfaces of the second invariant of the velocity gradient tensor (Q*=0.03) in the decaying homogeneous isotropic turbulence for the case of Re_λ =37.1. Second invariant Q is normalization by Kolmogorov microscale η and root mean square of velocity fluctuations, $u_{\rm rms}$.

Now in order to discuss about the characteristics of coherent fine scale eddy, at first, we notice the tube-like coherent fine scale eddy by visualization of flows in the DNS database. Figure 1 shows the contour surfaces of normalized second invariant of the velocity gradient tensor Q in the DNS data for Re_λ =37.1. The level of the isosurface is selected to be Q* =0.03. Hereafter, * denotes the normalization by Kolmogorov microscale η and root mean square of velocity fluctuations, $u_{\rm rms}$. The normalization of Q by η and $u_{\rm rms}$ is due to the fact that the diameter and the maximum azimuthal velocity of tube-like fine scale structures can be scaled by η and $u_{\rm rms}$[(10)-(12)]. In this figure, the visualized region is 1/8 of the whole calculation domain. Figure 1 shows that lots of coherent tube-like vortical structures are randomly oriented in homogeneous isotropic turbulence which demonstrates strong three-dimensional characteristics in turbulence. These tube-like vortical structures can be considered as the coherent fine scale eddy in turbulence. However, if we increase or decrease the value of Q*, we can also show distinct tube-like structures in turbulence, little bit different from Fig.1, which means the visualization of fine scale structures significantly depends on the thresholds value of Q[(10)-(14)]. However, in this case, we considered the threshold value of Q*=0.03 only to show the visualized structures in the flows. So it is necessary to consider an identification method that can educe fine scale eddy without choosing any thresholds of variables.

3.3 Details of the Identification Scheme

Since we use positive Q for visualization in Fig.1 and we can see the existence of many tube-like coherent structures in the DNS data in homogeneous isotropic turbulence. Obviously these tube-like eddies contain at least one local Q maximum on its axis. To identify the axes of fine scale eddy, first we search the points with local Q maximums on the cross-section of the axis of fine scale eddy. We consider this point as the starting point on the axis and from this point we move to the axial direction with a short distance to find the other point on the axis and continue this procedure until the end of the axis. The identification scheme consists of the following steps:

Step (a): Evaluation of Q at each collocation point from the results of DNS.

Step (b): Probability of existence of positive local maximum of Q near the collocation points is evaluated at each collocation point from Q distribution. Because the case that a local maximum of Q coincides with a collocation point is very rare, it is necessary to define probability on collocation points.

Step (c): Collocation points with non-zero probability are selected to survey actual maxima of Q. Locations of maximal Q are determined within the accuracy of 10^{-6} in terms of relative error of Q by applying a three dimensional cubic spline interpolation to DNS data.

Step (d): A cylindrical coordinate system (r, θ, z) is considered by setting the maximal point as the origin. The coordinate system is assumed to have advection velocity at the origin. The z direction is selected to be parallel to the vorticity vector at the maximal point. The velocity vectors are projected on this coordinate and azimuthal velocity u_θ is calculated.

Step (e): Point that has small variance in azimuthal velocity compared with the surroundings is determined. If the azimuthal velocities at r =1/5

computational grid space show same sign for all θ, that point is identified as the center of the swirling motion.

Step (f): Statistical properties are calculated around the points.

After completion of the above steps, we can get a point on the cross-section of the axis of coherent fine scale eddy with local Q maximum which is considered as the starting point ($\boldsymbol{x}_s$). From this starting point on the cross-section, axes of each coherent fine scale eddy are searched by using the following auto-tracing algorithm:

Step (g): From $\boldsymbol{x}_s$, the investigated point is moved in the axial direction with a short distance, $\boldsymbol{ds}$. $\boldsymbol{ds}$ is parallel to the vorticity vector at $\boldsymbol{x}_s$. A new cylindrical coordinate system (r', θ', z') is considered by setting the new point as the origin. On the (r', θ') plane with $z'=0$, the point with maximum Q is determined, and the steps (c)-(e) are applied.

Step (h): Central axis of each eddy is determined by repeating the step (g). In this procedure, $|\boldsymbol{ds}|$ is set equal to 1/5 computational grid space. If angle (ϕ_n) between $\boldsymbol{x}_{n-1}$ and $\boldsymbol{x}_n$ i.e., two neighboring points on the axis, is greater than 30 degree, the step (g) is applied again with $|\boldsymbol{ds}'| = |\boldsymbol{ds}|\cos(\phi_n).b$

Step (i): After the calculation of statistical properties, above steps are repeated until second invariant on the axis becomes negative or swirling motion can not be detected.

Step (j): The steps (g)-(i) are conducted in the opposite direction of vorticity vector at $\boldsymbol{x}_s$.

Step (k): The steps (g)-(j) are applied for the next starting point.

Detailed of this method is also given by Tanahashi et al. [11],[12] and Uddin et al.[13].

3.4 Axes of Coherent Fine Scale Eddy

The above identification method is applied in DNS results to educe the axes of fine scale eddy in homogeneous isotropic turbulence. Figure 2 displays the distributions of axes of coherent fine scale eddy for the case of Re_λ =37.1 in the same region which are shown in Fig.1. The view point of these two figures is same. The visualized width of the axes is drawn to be proportional to the square root of second invariant on the axis. By the comparison of figures 1 and 2, we can see the well coincidence of the identified axes and the tube-like eddies which are visualized by contour surfaces of Q. Figure 2 includes many weak eddies which are not visualized in Fig.1. This is because this identification does not depend upon the strength of the fine scale eddies in turbulence. This direct visualization of the axis gives only the information about spatial distribution of coherent fine scale eddy because the axis are defined as lines in three-dimensional field. However, the coherent fine scale eddy shows relatively large variance in their strength, length, etc. These variances are very important to understand the physics of turbulence. In our previous studies [11),(12)] we have shown that relatively large fluctuation of second invariant with several minima of Q occurs along the axis of fine scale eddy.

4. Three-dimensional Characteristics of the Fine Scale Eddy Along the Axis

We mentioned earlier that the coherent fine scale eddies show strong three-dimensional character as shown in Fig.1. To clarify the three-dimensional characteristics of coherent fine scale eddies, we have analyzed several fine scale eddies in homogeneous isotropic turbulence. In this section, we have selected three typical coherent fine scale eddies with different intensity for the case Re_λ =37.1. Here intensity of the coherent fine scale eddy is denoted by the value of Q on the axis.

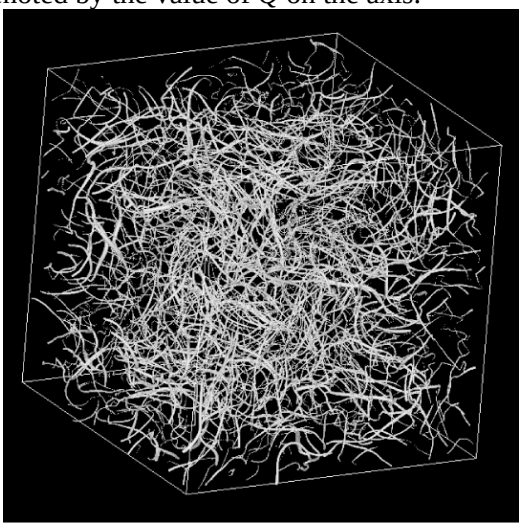

Fig. 2: The axes of coherent fine scale eddy for the case of Re_λ =37.1. The visualized width of the axes is drawn to be proportional to the square root of second invariant on the axis.

(a) Strong Eddy

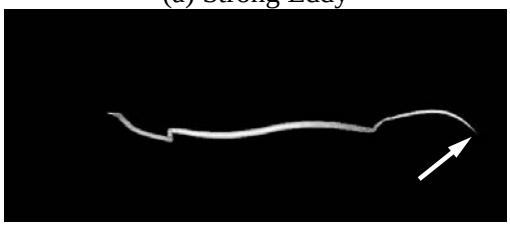

(b) Medium Eddy

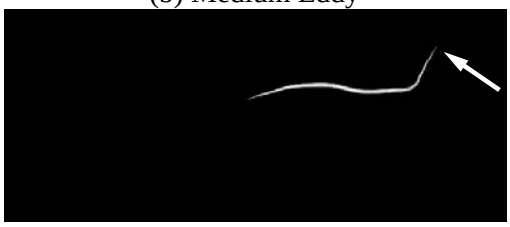

(c) Weak Eddy

Fig. 3: Axes of the typical coherent fine scale eddy. Thickness of the axis is proportional to the square root of second invariant on the axis of the eddy, $\sqrt{Q_c}$. (a) strong eddy, (b) medium eddy and (c) weak eddy. The arrow marked end of the axis indicates the origin.

Fig.3 shows the visualized axes of the selected typical eddy where (a) strong eddy, (b) medium eddy and (c) weak eddy in homogeneous isotropic turbulence. The visualized diameters of (a), (b) and (c) are selected to be proportional to the square root of second invariant Q on the axis. From Fig.3, we can see that the strong and medium eddies have several sharp bends that are identified with the minima of second invariant Q on the axis while a light bend exists in the weak eddy. It is also clear that the segments between the bends seem to show relatively large second invariant and to be nearly straight. From these figures, we can understand the three- dimensional characteristics of each eddy but these visualized figures are not sufficient to clarify its' significant character in turbulence. To understand the detailed structures of these fine scale eddies, we have calculated the following properties along the axis. Hereafter, the properties shown in (a), (b) and (c) of each figure given below, correspond to those given in Fig.3, respectively.

The distributions of second and third invariant of the velocity gradient tensor on the axes of the typical coherent fine scale eddy given in Fig.3 are shown in Figs.4 and 5, respectively. Here, asterisk denotes that the variables are normalized by Kolmogorov microscale, (η) and *r.m.s* of velocity fluctuations, (u_{rms}). s represents the coordinates along the axis and s_l and s_λ are normalized by integral length scale, (l) and Taylor microscale, (λ), respectively, where the selected origins of s are shown in Fig.3 by arrows. It is clear that the second invariant become negative at the end $s_l(s_\lambda)$ =0 for all cases given in Fig.4. At the other end, second invariant become negative for the cases of the medium and weak eddies, whereas distinct swirling motion can not be observed for the case of the strong eddy (Fig. 4(a)). Because of the above reason, we have stopped the identification procedure. From the relation between second invariant Q and coordinate s, we can find the length of the coherent fine scale eddies in turbulence. In the present cases, the length of the strong eddy reaches to $2.4l$, 12.3λ and 148η and for the case of the medium eddy it is $1.4l$, 7.1λ and 85η. On the other hand, the length of the weak eddy is only $0.6l$, 3.1λ and 37η. Previously, it is reported that the length of the tube-like structures appears to be of the order of integral length scale[6],[8],[21]. In their studies, mainly the strongest structures are considered. Whereas, in this study, it is possible to characterize all eddies in turbulence as we can see in Fig.4.

From the distributions of Q, we can see that relatively large fluctuation of Q occurs along the axis of fine scale eddies and several minima of Q exist along it. In this study, we defined the 'nodes' of the eddy with the minima of second invariant on the axis. It shows clearly that the strong eddy has 4 nodes and medium eddy has 2 nodes while a single node is contained by the weak eddy.

The signs of the third invariant of the velocity gradient tensor represent the local stretching and compression of fluid element[19]. As we can see from Fig.5, third invariant show negative values in most of the part of the axes, which imply that these eddies are continuously stretched along its axes. It is also clear that the stretching rate on

the axis decreases at the nodes of fine scale eddies because the third invariant seems to increase there. The pattern is almost opposite in the profiles of Q and R given in Figs.4 and 5, respectively.

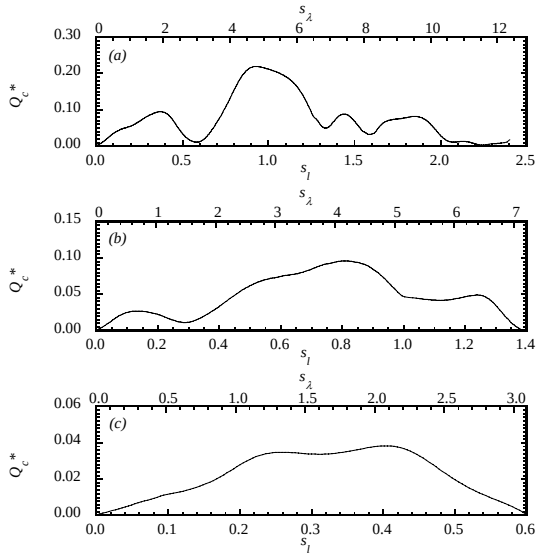

Fig. 4: Distributions of second invariant on the axes of the typical coherent fine scale eddy. Second invariant Q is normalized by η and u_{rms}. s is the coordinates along the axes and s_l and s_λ are normalized by integral length scale, l and Taylor microscale, λ, respectively. (a) strong eddy, (b) medium eddy and (c) weak eddy.

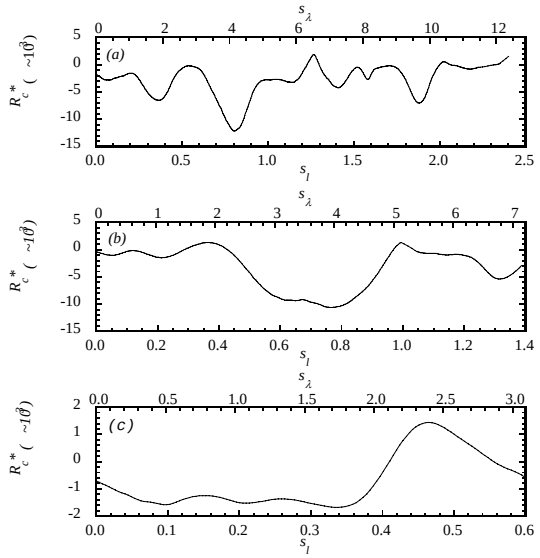

Fig. 5: Distributions of third invariant on the axes of the typical coherent fine scale eddy. Third invariant R is normalized by η and u_{rms}. (a) strong eddy, (b) medium eddy and (c) weak eddy.

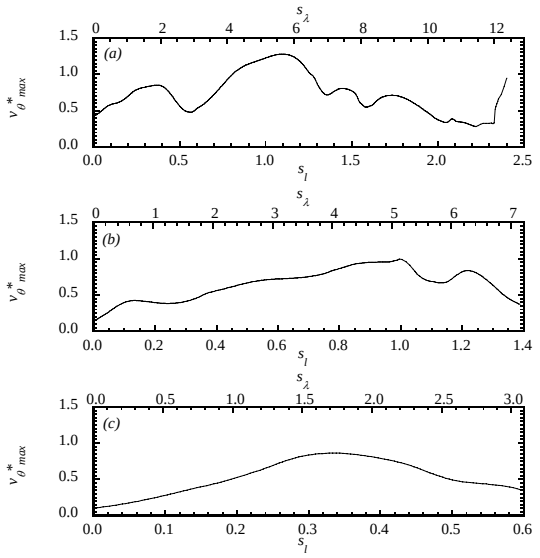

Fig.6: Distributions of maximum azimuthal velocity along the axes of the typical coherent fine scale eddy normalized by u_{rms}. (a) strong eddy, (b) medium eddy and (c) weak eddy.

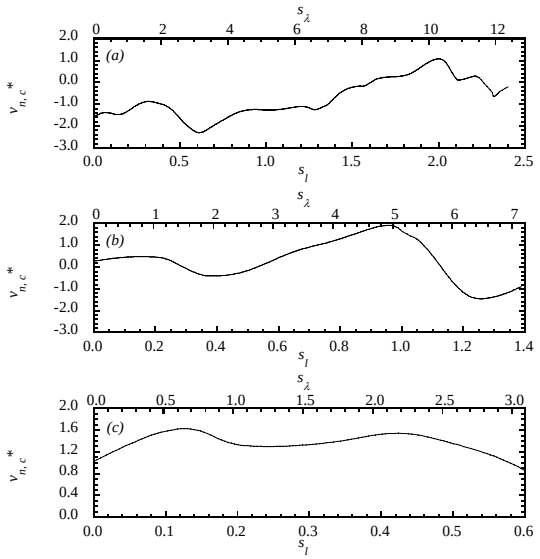

Fig. 7: Distributions of axial velocity along the axes of the typical coherent fine scale eddy normalized by u_{rms}. (a) strong eddy, (b) medium eddy and (c) weak eddy.

Figs.6 and 7 show the distributions of maximum azimuthal velocities on the cross-section and axial velocities on the axis of the typical coherent fine scale eddies given in Fig.3, respectively. These velocity profiles are normalized by u_{rms}. The azimuthal velocity of the coherent fine scale eddy is of the order of u_{rms} which is also shown in previous research by Tanahashi et al.[10][11]. The fluctuations of maximum azimuthal velocities along the axes

are well correlated with that of second invariant given in Fig.4. It is revealed that the sections with large second invariant show relatively large azimuthal velocities along the axis, while the fluctuation of axial velocity is not so large. We can observe very strong axial flows with positive and negative velocities in the case of strong and medium eddy but weak eddy shows only positive velocity in axial direction. The magnitude of axial velocity component is relatively large and is of the order of u_{rms}.

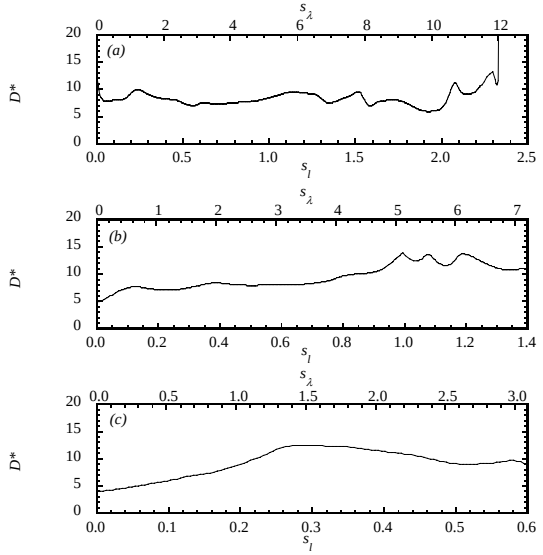

Fig. 8: Distributions of diameter along the axes of the typical coherent fine scale eddy. The diameter is normalized by η. (a) strong eddy, (b) medium eddy and (c) weak eddy.

Fig. 8 gives the distributions of diameter along the axes of the typical coherent fine scale eddy. The diameter is normalized by Kolmogorov microscale (η). In this study, radius of the fine scale eddy is defined by a distance between the center and location where the mean azimuthal velocity reaches to the maximum value. Contrary to the large fluctuation of second invariant and maximum azimuthal velocity, the variation of diameter along the axes is very small. Figs.8(b) & (c) show that the diameter is about 5η at the origin but gradually increases to 8η. Nevertheless, the most expected diameter of the coherent fine scale eddy is nearly constant along the axis and about 8-9η. The mean diameter of the coherent fine scale eddies would be 8-10η that is very close to the value reported by Tanahashi et al.[10],[11].

Fig. 9 gives the inclination angle (ϕ) which is integrated from the origin. The axes of coherent fine scale eddy turn its' direction at the nodes where second invariant is minimum. We have seen that the segments of axes between the nodes are nearly straight but the axis bends with a large angle, almost π, at the nodes. However, the inclination angle of the weak eddy, Fig.9(c), is relatively small.

We have seen in Figs.1 and 2 that the coherent fine scale eddies show strong swirling motion around its' axes and have distinct three dimensional characters. These eddies are continuously moving with large advection velocity in turbulence[11].

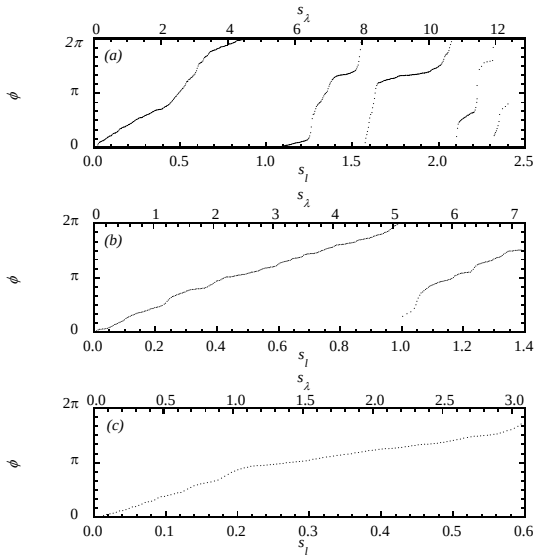

Fig. 9: Inclination angle of the axes of the typical coherent fine scale eddy. (a) strong eddy, (b) medium eddy and (c) weak eddy.

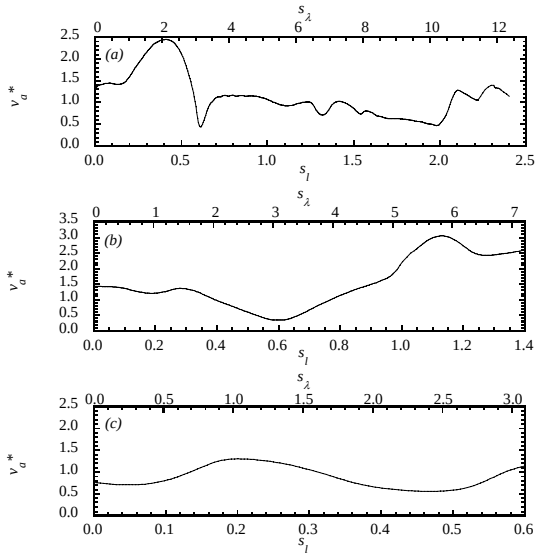

Fig. 10: Magnitude of the advection velocity in the radial direction of the typical coherent fine scale eddies. The magnitude of the advection

velocity is normalized by u_{rms}. (a) strong eddy, (b) medium eddy and (c) weak eddy.

The magnitudes of advection velocity in the radial direction of the given typical coherent fine scale eddies on each section are shown in Fig.10. The total advection velocity of the fluid elements near the central axis can be represented by sum of axial velocity given in Fig.7 and the radial advection velocity given in Fig.10. However, we discuss only the radial advection velocity because the axial velocity on the axis does not correspond to the advection of the eddy if the coherent fine scale eddy can be locally approximated by a Burgers' vortex. In the case of stretched Burgers' vortex, the outer strain field induces axial velocity, while the vortex has no advection velocity. Fig.10 suggests that the advection velocity of the axes is also the order of u_{rms}.

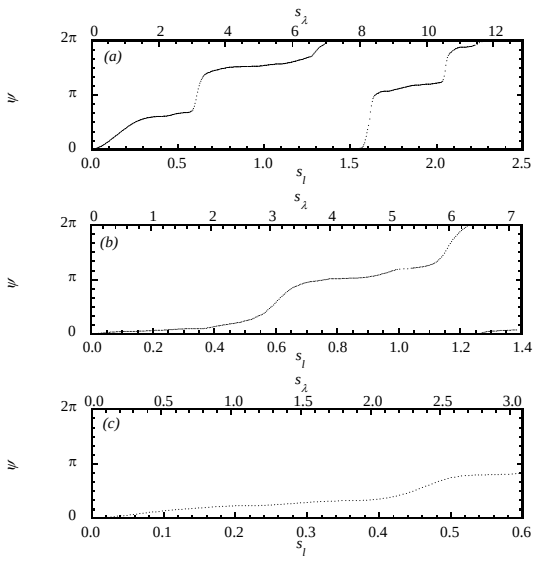

Fig. 11: Direction angle of the advection velocity of the typical coherent fine scale eddies. (a) strong eddy, (b) medium eddy and (c) weak eddy.

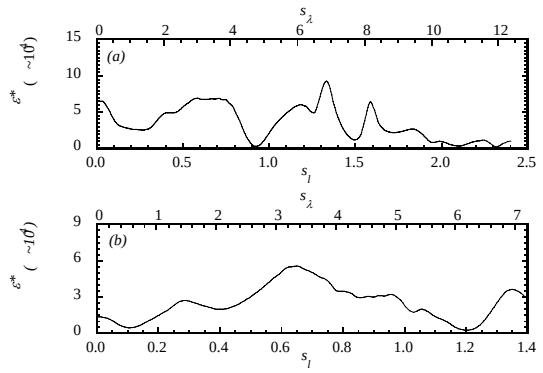

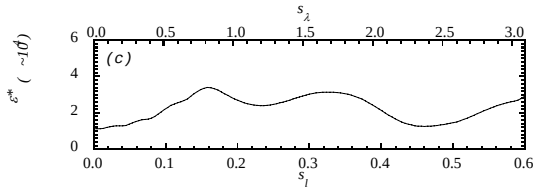

Fig. 12: Distributions of dissipation rate on the axes of the typical coherent fine scale eddy. Dissipation rate, ε is normalized by η and u_{rms}. (a) strong eddy, (b) medium eddy and (c) weak eddy.

Fig. 11 gives the direction angle of advection of the typical eddies in a (r, θ)-plane. The change of advection direction of the weak eddy is very small and it also shows almost uniform advection velocity around its entire axis. On the other hand, strong and medium eddies drastically change its' direction of advection at every nodes and these angles are the order of π similar to the inclination angle given in Fig.9, while the magnitude of advection velocity and the direction are nearly uniform in the segments between the nodes. These results imply that segments of the coherent fine scale eddies which are divided by the nodes are moving in the other directions, respectively.

Coherent fine scale eddy plays an important role in the total turbulent energy dissipation and its intermittent character[(11),(12),(22)]. Tanahashi et al.[(11),(12),(22)] have shown that turbulent energy dissipation near the center of vortex tube is very small while the energy dissipation is large in the negative second invariant region. Figure12 shows the distributions of dissipation rate (ε) on the central axes of coherent fine scale eddy which is normalized by η and u_{rms} where,

$$\varepsilon = 2\nu S_{ij} S_{ij} \qquad (6)$$

From the profiles of Fig.12 it is revealed that the dissipation rate on the central axes of the fine scale eddy is not so large along the axis and the value of it also depends on the second invariant and size of the eddy. In Fig.5 we have seen that the above coherent fine scale eddies give the negative third invariant in the most part on its axes and from Fig.12 we can see that the dissipation rate is relatively large in negative third invariant region of coherent fine scale eddies. Also the dissipation becomes relatively large at the nodes of the eddy.

4. Mean Characteristics of The Fine Scale Eddy Around The Axis

In this section, we present the mean characteristics of fine scale eddy around its' axes as a function of radius.

Fig. 13 and 14 show the mean distributions of normalized second and third invariant around the axes of fine scale eddy given in Fig.3. Here, *r* indicates the radius of the tube-like fine scale eddy.

From Fig. 13 we can see the existence of relatively large second invariant on the axis and it gradually decreases towards the ambient of the tube-like fine scale eddies, and finally it becomes negative. In the case of weak eddy, we can observe the existence of large second invariant far from the axis, which imply that the other eddy may intersect there. We can see from Fig.14 that the typical fine scale eddies in the present study show the negative values not only on the axis but also around the axis of it. At the nodes, mentioned earlier, third invariant gives the positive value. As the negative third invariant represents the stretching character of fine scale eddies, the given strong eddies (Fig.14 (a&b)) are undoubtedly stretched in the turbulence. In the case of weak eddy (Fig.14(c)), most of the part on the axis shows negative values but around the axis about half of the region shows positive values.

Fig.s15-17 show the mean distributions of normalized velocities around the typical axes given in Fig.3, respectively. Here Fig.15 gives the mean azimuthal velocity, Fig.16 represents the mean radial

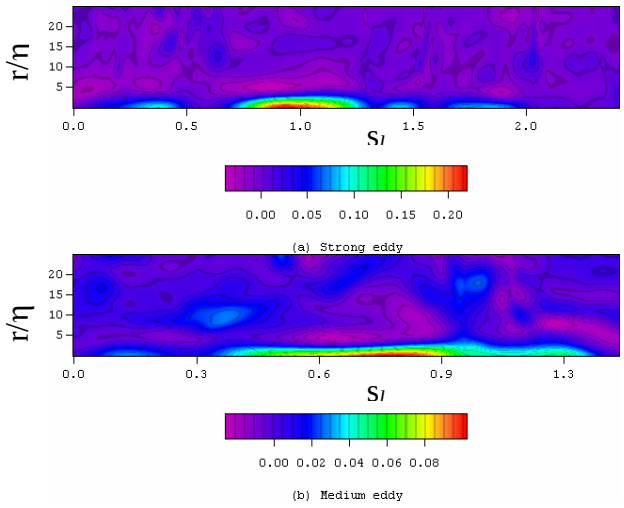

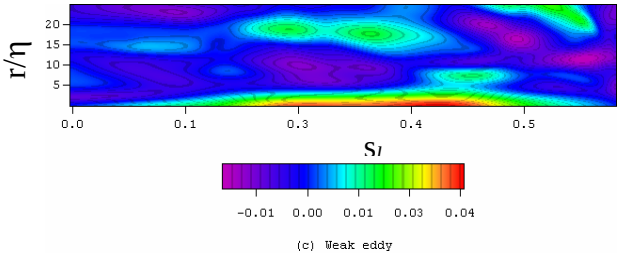

Fig. 13: Mean distributions of second invariant along the coherent fine scale eddies. *r* represents the radius and *s* is the coordinate along the axes.

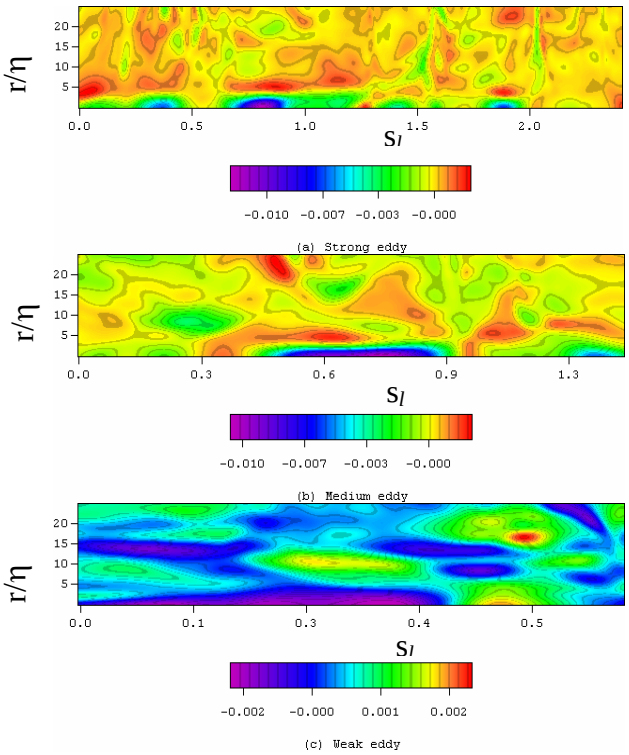

Fig. 14: Mean distributions of third invariant along the coherent fine scale eddies. *r* represents the radius and *s* is the coordinate along the axes.

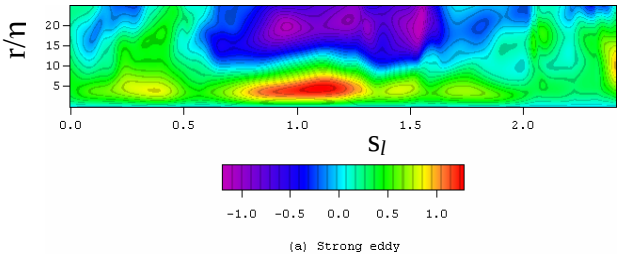

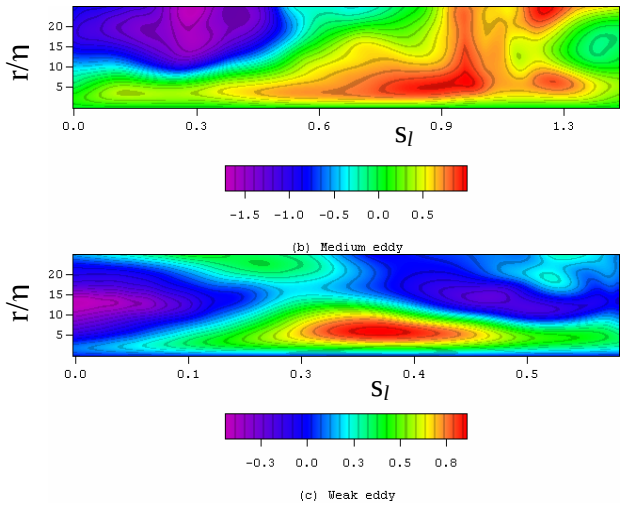

Fig. 15: Mean distributions of azimuthal velocity along the coherent fine scale eddies. *r* represents the radius and *s* is the coordinate along the axes.

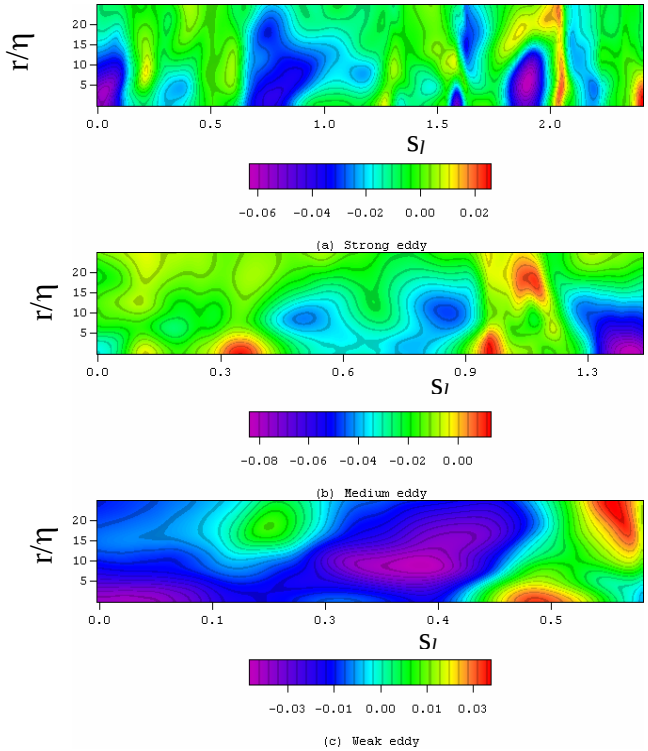

Fig. 16: Mean distributions of radial velocity along the coherent fine scale eddies. *r* represents the radius and *s* is the coordinate along the axes.

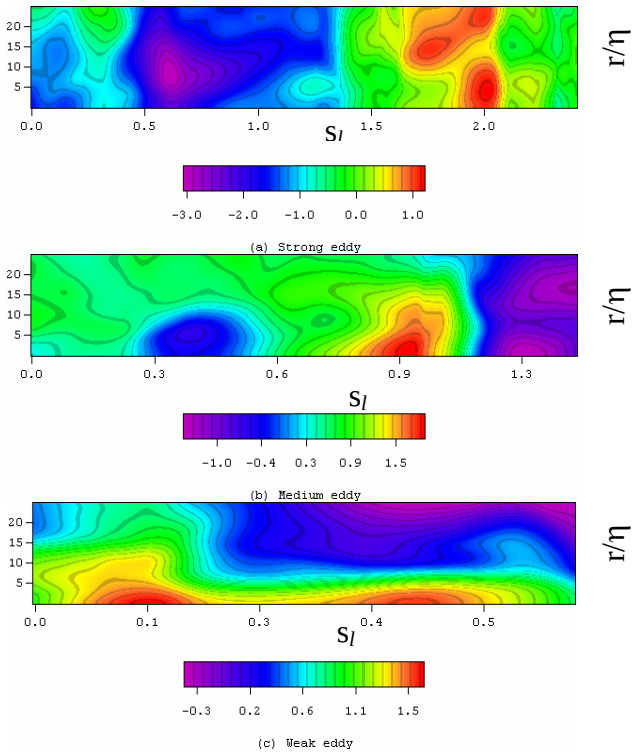

Fig. 17: Mean distributions of axial velocity along the coherent fine scale eddies. *r* represents the radius and *s* is the coordinate along the axes.

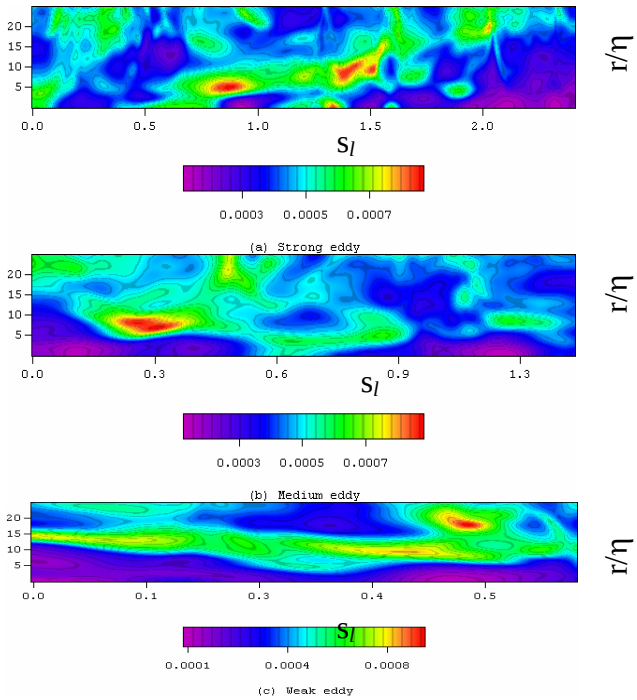

Fig. 18. Mean distributions of dissipation rate along the coherent fine scale eddies. *r* represents the radius and *s* is the coordinate along the axes.

velocity and Fig.17 shows the mean axial velocity around the axes of coherent fine scale eddy. The distributions of mean azimuthal velocity of fine scale eddies provide the evidence of existence of the distinct swirling motion around the axes of coherent fine scale structure in turbulence. Coherent fine scale eddies produce strong rotational motion in the area where second invariant Q is large. Also relatively strong flow can be observed toward the central axis of fine scale eddy. There are strong radial flows from the ambient of the tube-like eddy to the central axis. The uniform incoming flow can be observed where the second invariant is large or the segments between the nodes of the axis. Fig.17 suggests that the very strong axial flows can be observed not only on the axis of fine scale eddies but also in the regimes far from the central axis. In the case of strong eddy (Fig.17(a)), we can see that the axial flow is divided into negative and positive parts at about s_l =1.4 and shows the same pattern in the respective parts not only on the axis but also in the entire regime around its axis. On the other hand, the weak eddy (Fig.17(c)) shows only positive flows on the axis throughout its whole length and negative flows far from the central axis.

Fig. 18 shows the distribution of mean energy dissipation along the axis of fine scale eddies given in Fig.3, respectively. The maxima of mean energy dissipation rate averaged in the azimuthal direction reaches to twice of volume-averaged value. The coherent fine scale eddies have important role in the dissipation of turbulent energy and its intermittent character[(11)]. In this study, we have restricted our discussion to the above three typical coherent fine scale eddies. We applied the same analysis for lots of individual coherent fine scale eddies and have observed that the characteristics of other eddies are quite similar to the above. We are confirmed that the three-dimensional features of tube-like fine scale eddies should follow the above characteristics in turbulence.

5. Conclusions

In this study, we have presented the detailed structures of several typical coherent fine scale eddy related to its' axis in homogeneous isotropic turbulence with its mean characters around the axis. The following conclusions can be drawn from our observation. The axes of coherent fine scale eddy have several nodes, which are identified by the minima of second invariant of the velocity gradient tensor on the axis. The number of nodes increases for strong or relatively long eddy but it decreases for weak or short eddy. The sections of fine scale eddy between two consecutive nodes show relatively large second invariant and are nearly straight.

The maximum azimuthal velocity and axial velocity of coherent fine scale eddy show relatively large fluctuations along the axes, while the diameter is nearly constant along the entire axis of fine scale eddy.

At each node, the axis bends with a large angle. Magnitude of advection velocity and directional movement of the coherent fine scale eddy also change at the nodes of the axis.

The coherent fine scale eddies have strong axial flow and large advection velocity, which suggest that the streamlines of the flow can not represent swirling motion of the coherent fine scale eddy.

The dissipation rate along the axes of fine scale eddy is not so large but the fine scale eddy produces high-energy dissipation around the axis of it. Also the axis of fine scale eddy shows relatively higher dissipation rate at the nodes of the axis.

References

[1] Tennekes, H., Simple model for the small-scale structure of turbulence, Phys. Fluids, Vol. 11, No. 3, (1968) pp. 669-761.

[2] Lundgren, T. S., Strained spiral vortex model for turbulent fine structure, Phys. Fluids, Vol. 25, (1982) pp. 2193-2203.

[3] Pullin, D. I. and Saffman, P. G., On the Lundgren-Townsend model of turbulent fine scales, Phys. Fluids, Vol. A5, (1993) pp.126-145.

[4] Saffman, P. G. and Pullin, D. I., Anisotropy of the Lundgren-Townsend model of fine-scale turbulence, Phys. Fluids, Vol. A6, (1994) pp. 802-807.

[5] She, Z. –S., Jackson, E. and Orszag, S. A., Intermittent vortex structures in homogeneous isotropic turbulence, Nature, Vol. 344, (1990) pp. 226-228.

[6] Vincent, A. and Meneguzzi, M., The spatial structure and statistical properties of homogeneous turbulence, J. Fluid Mech., Vol. 225, (1991) pp.1-20.

[7] Vincent, A. and Meneguzzi, M., The dynamics of vorticity tubes in homogeneous turbulence, J. Fluid Mech., Vol. 258, (1994) pp. 245-254.

[8] Jimenez, J., Wray, A. A., Saffman, P. G. and Rogallo, R. S., The structure of intense vorticity in isotropic turbulence, J. Fluid Mech., Vol. 255, (1993) pp.65-90.

[9] Kida, S., Tube-like structure in turbulence, Lecture Notes in Num. Appl. Anal., Vol. 12, (1993) pp.137-159.

[10] Tanahashi, M., Miyauchi, T. and Iwase, S.,

Statistics of coherent fine scale structure in homogeneous isotropic turbulence", Bulletin of the American Physical Society, Vol. 43, No. 9, (1998) pp. 1975.

[11] Tanahashi, M., Uddin, M. A., Iwase, S. and Miyauchi, T., Three dimensional feature of coherent fine scale eddies in homogeneous isotropic turbulence, Trans. JSME, Vol. 65(B), No. 638, (in Japanese) (1999) pp.3237-3243.

[12] Tanahashi, M., Iwase, S., Uddin, M. A. and Miyauchi, T., Three dimensional features of coherent fine scale eddies in turbulence, Turbulence and Shear Flow Phenomena-1(4), (1999) pp.79-84.

[13] Uddin, M. A., Tanahashi, M., Iwase, S. and Miyauchi, T., Visualization of axes of coherent fine scale eddies in homogeneous isotropic turbulence, Proc. of the 3rd Pacific Symposium on Flow Visualization and Image Processing (PSFVIP-3), CD-ROM Proc., C3-2, F3204 (2001), pp.1-7.

[14] Uddin, M. A., Kato, C., Yamade, Y., Ohshima, N., Tanahashi, M. and Miyauchi, T., Large eddy simulation of homogeneous isotropic turbulent flow using the finite element method, JSME Int. J, Ser. B, Vol. 49(1) (2006), pp.102-114.

[15] Tanahashi, M., Miyauchi, T. and Matsuoka, K., Coherent fine scale structures in temporally developing turbulent mixing layers, Proc. of 2nd Int. Symp. on Turbulence, Heat and Mass Transfer, Vol. 2, (1997) pp.1256-1261.

[16] Tanahashi, M., Das, S. K., Shoji, K. and Miyauchi, T., Coherent fine scale structure in turbulent channel flows. Trans. JSME, Vol. 65(B), No. 638, (in Japanese) (1999) pp.3244-

[17] Tanahashi, M., Tsujimoto, T, Karim, M. F., Fujimura, D. and Miyauchi, T., Anisotropy of MHD homogeneous turbulence (2nd report, coherent fine scale eddies and Lorentz force), Trans. JSME, Vol. 65(B), No. 640, (in Japanese) (1999) pp.3884-3890.

[18] Jeong, J. and Hussain, F., On the identification of a vortex, J. Fluid Mech., Vol. 285, (1995) pp.69-94.

[19] Chong, M. S., Perry, A. E. and Cantwell, B. J., A general classification of three-dimensional flow field. Phys. Fluids A2, (1990) pp.765-777.

[20] Tanahashi, M., Iwase, S., Uddin, M. A., Takata, N. & Miyauchi, T., Distribution of coherent fine scale eddies and turbulent heat transfer in homogeneous isotropic turbulence, Thermal Science and Engineering, Vol. 8, No. 3, (2000) pp.29-38.

[21] Nomura, K. K. and Post, G. K., The structure and dynamics of vorticity and rate of strain in incompressible homogeneous turbulence. J. Fluid Mech., (1998), Vol. 377, pp. 65-97.

[22] Tanahashi, M., Miyauchi, T. and Yoshida, T., Characteristics of small scale vortices related to turbulent energy dissipation, Proc. of 9th Int. Symp. on Transport Phenomena in Thermal Fluid Engineering, Vol. 2, (1996) pp.1256-1261.